The Journal of Experimental Biology 207, 2577-2588
Published by The Company of Biologists 2004
doi:10.1242/jeb.01065

Ontogenetic patterns of limb loading, *in vivo* bone strains and growth in the goat radius

Russell P. Main* and Andrew A. Biewener

Concord Field Station, Department of Organismic and Evolutionary Biology, Harvard University, 100 Old Causeway Road, Bedford, MA 01730, USA

*Author for correspondence (e-mail: rmain@oeb.harvard.edu)

Accepted 30 April 2004

Summary

As tetrapods increase in size and weight through ontogeny, the limb skeleton must grow to accommodate the increases in body weight and the resulting locomotor forces placed upon the limbs. No study to date, however, has examined how morphological changes in the limb skeleton during growth reflect ontogenetic patterns of limb loading and the resulting stresses and strains produced in the limbs. The goal of this study was to relate forelimb loads to *in vivo* bone strains in the radius of the domestic goat (*Capra hircus*) across a range of gaits and speeds through ontogeny while observing how the growth patterns of the bone relate to the mechanics of the limb. *In vivo* bone strains in the radius were recorded from two groups of juvenile goats (4 kg, 6 weeks and 9 kg, 15 weeks) and compared with previously reported strain data for the radius of adult goats. Ontogenetic strain patterns were examined in relation to peak forelimb ground reaction forces, ontogenetic scaling patterns of cross-sectional geometry and bone curvature, and percentage mineral ash content. Peak principal longitudinal tensile strains on the cranial surface and compressive strains on the caudal surface of the radius increased during ontogeny but maintained a uniform distribution, resulting in the radius being loaded primarily in bending through ontogeny. The increase in strain occurred despite uniform loading (relative to body weight) of the forelimb through ontogeny. Instead, the increase in bone strain resulted from strong negative growth allometry of the cross-sectional area ($\propto M^{0.53}$) and medio-lateral and cranio-caudal second moments of area ($I_{ML} \propto M^{1.03}$, $I_{CC} \propto M^{0.84}$) of the radius and only a small increase (+2.8%) in mineral ash content. Even though bone strains increased with growth and age, strains in the younger goats were small enough to suggest that they maintain safety factors at least comparable with adults when moving at similar absolute speeds. Increased variability of loading in juvenile animals may also favor the more robust dimensions of the radius, and possibly other limb bones, early in growth.

Key words: bone geometry, bone growth, bone strain, limb loading, ontogeny, scaling.

Introduction

Of the tetrapod limb bones examined to date, many appear to be designed in a way that maintains peak locomotor bone strain magnitudes similarly across a broad taxonomic scale and a large size range of animals. Peak strain magnitudes in a wide diversity of adult tetrapod limb bones, from horses and pigeons to alligators and bats, range between –1800 to –3000 microstrain (Rubin and Lanyon, 1982; Biewener and Taylor, 1986; Swartz et al., 1992; Biewener and Dial, 1995; Blob and Biewener, 1999), indicating safety factors of between two and four for most of the taxa examined to date (Alexander, 1981; Biewener, 1989). This broad strain similarity occurs in birds and mammals even though the dimensions of their limb bones scale with isometry or only slight positive allometry (Alexander et al., 1979; Maloiy et al., 1979; Biewener, 1982), rather than the strong positive allometry needed to maintain strain similarity. These conflicting results led Biewener (1983, 1989) to propose that peak strain levels and similar safety factors in mammals are in part maintained over their size range because larger mammals have a more upright posture and less curved long bones leading to reduced relative bending loads in support of the animal's weight during locomotion.

Although these studies and the ideas they espouse have contributed greatly to the understanding of form and function in the musculoskeletal system, they are limited in their broad taxonomic comparison made over a large size range of adult organisms. The strategies used to maintain bone stresses within safe limits in the limbs of animals that vary over a smaller size range and that are more closely related may be different from those seen in general comparisons of more distantly related taxa. One example in which this may be the case is during the ontogenetic growth of an animal, for which negative allometry in the cross-sectional geometry and other linear dimensions of limb bones has been reported (Carrier, 1983; Carrier and Leon, 1990; Biewener and Bertram, 1994).

In the black-tailed jack rabbit (*Lepus californicus*), negative allometry of the diameter and second moment of area of the third metatarsal allows for relatively lower stresses in the bones of younger rabbits, which are less well mineralized and therefore not as stiff as the bones of older rabbits (Carrier, 1983). Carrier proposed that these features, coupled with appropriate changes in the moment and contractile properties of the gastrocnemius, allowed younger and older rabbits to maintain a similar capacity for accelerating and escape velocity through much of ontogeny. Although Carrier's study argued for a selective advantage in the departure away from the positive skeletal allometry needed to maintain stress/strain similarity in the rabbit's limb bones, his analysis was largely based on morphometric data and did not quantify features of *in vivo* locomotor performance and mechanics that would allow the actual stresses and strains on the musculoskeletal system of growing jack rabbits to be determined.

Related studies examining bone strains (Biewener et al., 1986) and morphological scaling patterns in the chicken tibiotarsus (Biewener and Bertram, 1994) during ontogenetic growth found that even though the tibiotarsus showed negative ontogenetic allometry in both cross-sectional and second moments of area, peak strains (assessed at 35% of maximum speed) in the tibiotarsus remained constant during most of the animal's growth. However, in contrast to the suggested similarity in peak bone stresses at absolute levels of locomotor performance (e.g. peak acceleration) indicated for growing jack rabbits (Carrier, 1983), the results for the chicken tibiotarsus indicate that locomotor stresses/strains were not maintained through ontogeny at similar absolute speeds. Peak bone strains remained similar between 4- and 17-week-old chickens at the same relative speeds (0.48 m s^{-1} and 1.17 m s^{-1}, respectively). However, this suggests that if young chicks approached adult speeds, bone strains would probably exceed adult strain levels despite younger chicks having relatively more robust tibiotarsi. These studies focused on linking patterns of bone strain to changes in bone geometry during skeletal growth but did not examine how limb and bone loading patterns may be related to locomotor performance and resulting levels of bone strain. No study to date, therefore, has examined how bone strain patterns and ontogenetic changes in bone size and shape relate to the locomotor forces transmitted by the limb as an animal grows. By linking ontogenetic patterns of limb loading with patterns of bone geometry and functional strain magnitudes, two important questions can be addressed: (1) how is skeletal growth matched to increases in body mass and limb loading and (2) does this interaction result in similar patterns and magnitudes of functional bone strains during ontogeny, as has been previously observed in the chicken tibiotarsus (Biewener et al., 1986)?

To answer these questions, we collected forelimb loading data and *in vivo* bone strains from the goat radius through ontogeny across a range of gaits and speeds. We also collected morphometric data to determine how the midshaft cross-sectional geometry of the radius changed during ontogenetic growth. We hypothesized that (1) strain magnitudes and distributions at the midshaft of the goat radius would remain relatively constant across different age and size groups within a given gait, similar to the chicken tibiotarsus. Consistent with this hypothesis, but in contrast to the findings of previous ontogenetic skeletal allometry studies (Carrier, 1983; Biewener and Bertram, 1994), we (2) expected that bone growth patterns would match changes in limb loading with positive allometry in bone cross-sectional geometry and decreased longitudinal curvature to maintain ontogenetic strain similarity. We also hypothesized that (3) the radius would be loaded primarily in bending during stance throughout ontogeny at all gaits, similar to the pattern observed previously in adult goats (Biewener and Taylor, 1986).

Materials and methods

Animals

Domestic goats (*Capra hircus* L.) were obtained from a breeding population housed at the Concord Field Station in large outdoor paddocks. Animals in three size classes were studied. Animals were grouped by size ('small', <6 kg; 'intermediate', 6–11 kg; 'adult', >15 kg) rather than by age due to size variation among individuals at a given age and because we consider size to be the critical determinant of limb and bone loading. Nevertheless, differentiation by size also generally separated the goats by age.

Ground reaction force (GRF) data were collected from six small young goats (mass, 4.3±1.2 kg; age, 5.6±4.0 weeks; mean ± S.D.), seven intermediate goats (mass, 8.7±1.6 kg; age, 15.2±10.4 weeks) and five large adult goats (mass, 31.7±11.3 kg; age, 3.0±2.4 years) over a range of gaits and speeds. *In vivo* strain data were recorded from the midshaft radius of the same six small and seven intermediate goats across speed and gait (Table 1) and compared with previously published data for three adult goats (mass, 27.0±2.65 kg; age, >2 years; Biewener and Taylor, 1986). Similar methods to collect the strain data were used here as in the earlier study, except that in the present study strains were measured from the medial surface of the radius, in addition to the cranial and caudal surfaces. Also, strains were not measured from the tibia. Bone geometry and percentage mineral ash content data were collected from 11 small (mass, 3.7±1.5 kg; age, 5.1±5.4 weeks), eight intermediate (mass, 8.7±3.0 kg; age, 17.4±11.4 weeks) and four adult goats (mass, 20.3±5.2 kg; ages, 0.8, 0.8, 1.2 and 7.0 years). Morphological measurements were obtained from the juvenile animals in which strains were collected, as well as from four adult goats euthanized for other purposes and six additional goats (1.5–8.8 kg) that died of natural causes.

Ground reaction force data collection

GRF data were collected to examine how peak limb loads changed through ontogeny between the different groups. They were also recorded before and after the surgery to attach the strain gauges in the juvenile goats to determine if GRFs were diminished as a result of any post-surgical lameness. Before the

GRF data were collected, both forelimbs were shaved, the centers of joint rotation palpated and the following points marked with non-toxic white paint: top of the scapula, shoulder, elbow, wrist, metacarpo-phalangeal joint and hoof. The distances (segment lengths) between the markers were also recorded.

The GRF data were recorded using a Kistler force platform (0.4 m×0.6 m; 9286A; Kistler, Amherst, NY, USA) and an A/D converter (Bioware 3.2; Kistler) sampling at 2.5 kHz. The goats were simultaneously videotaped from a lateral view (Redlake Motionscope PCI; San Diego, CA, USA) at 125 Hz to record which limbs made contact with the plate, the timing of foot contact and to ensure that only data from trials in which the goat was moving at a steady speed were analyzed. A post-trigger pulse that stopped the video camera was also recorded by the computer to synchronize the force and video data. The magnitude of the peak vertical GRF was measured and normalized by the goat's body weight ($\mathbf{F}_V/BW$) to assess ontogenetic patterns of limb loading.

Surgical procedures

The day following the pre-surgical force platform and video recordings, goats were prepped for surgery and anesthetized using a mixed injection of xylazine (1 mg kg^{-1}) and ketamine (4 mg kg^{-1}) into the jugular vein. After induction, goats were intubated and maintained on a closed system anesthesia machine (Matrx, Orchard Park, NY, USA) at 0.5–1.0% isoflurane. Breathing and heart rate were monitored throughout surgery and the anesthesia was adjusted as necessary.

Strain gauges were attached under sterile surgical conditions to the cranial, caudal and medial midshaft surfaces of the left radius. A 3–5 cm incision was made over the medial surface of the radius. After exposing the attachment sites by retracting the skin and overlying muscles, a small 1 cm^2 region of the periosteum was removed and the underlying mineralized surface lightly scraped with a periosteal elevator. The bone surface was then defatted and dried using methyl ethyl ketone (Sigma Chemical Co., St Louis, MO, USA). Once dried, the gauges were attached to each bone site using a self-catalyzing cyanoacrylate adhesive (Duro, Henkel Loctite Corp., Rocky Hill, CT, USA).

Sterilized rectangular rosette strain gauges (FRA-1-11; Tokyo Sokki Kenkyujo Co., Ltd, Tokyo, Japan) were attached to both the cranial and caudal surfaces of the radius while a single element gauge (FLA-1-11) was attached medially. Rosette strain gauges are three-element gauges that allow the maximum (tensile) and minimum (compressive) principal strains, and their angles (ϕ) relative to the bone's longitudinal axis to be determined. The rosette gauges were attached so that the central element of the gauge was aligned closely parallel to the bone's longitudinal axis at each site. The actual position and angular orientation of the strain gauges were determined post-mortem using a clear protractor and ruler. On average, alignment of the gauges was within ±3° (range, 0–15°) to the bone's longitudinal axis, with the gauges' proximo-distal position at the midshaft varying by less than 6±5% of the bone's length.

After the strain gauges were bonded to the bone's three midshaft surfaces, the medial incision was sutured and the wire leads (36-gauge, etched Teflon insulation; Micromeasurements, Raleigh, NC, USA) passed through the distal end of the sutured incision. The lead wires were then wrapped laterally around the limb and the pre-soldered epoxy-mounted miniature connector (3xGM-6; Microtech, Inc., Boothwyn, PA, USA) sutured to the skin to provide strain relief to the wires. The incision and the connector were then wrapped in sterile gauze and elastic bandaging tape.

Strain data collection

The goats were given 1–2 days to recover following surgery. If they showed any visible signs of lameness during recovery, an intramuscular injection of flunixin (1 mg kg^{-1}) was administered every 12 h to relieve soreness in the limb. The lead wire connector for the strain gauges was connected to a 5.5 m shielded cable (NMUF6/30-4046SJ; Cooner Wire, Chatsworth, CA, USA) that was secured with surgical tape to the upper part of the forelimb and to a collar around the goat's neck. The cable connected to a bridge amplifier (Vishay 2120; Micromeasurements), from which the raw strain signals were sampled by an A/D converter (Axon Instruments, Union City, CA, USA) at either 1.0 or 2.5 kHz. The goat's joint centers and hoof were again marked, and lateral-view video was collected at 125 Hz and synchronized to the strain data using a trigger pulse to relate the timing of foot contact, stride length, stride frequency and duty factor to the bone strain recordings.

Data were collected while the goats were run down a hallway (small, N=4; intermediate, N=6) or on a motorized treadmill (small, N=3; intermediate, N=2). For the hallway trials, speed was determined by digitizing the eye of the animal as it moved through the field of view. Hallway over-ground recordings provided an assessment of bone strain patterns recorded under equivalent circumstances as our force platform recordings. However, treadmill recordings provided steadier speeds and allowed a larger number of strides over a wider range of speeds and gaits to be collected. No significant differences in strains were found at any site for any speed or gait during treadmill *versus* over-ground locomotion in the two goats for which equivalent recordings were made (Student's paired t-test, P>0.05). After *in vivo* bone strain and post-surgical GRF data collection was completed, each goat was euthanized by an injection of sodium pentobarbital (150 mg kg^{-1}; intravenous, jugular), and their limb bones dissected for morphological and histological analysis.

Strain data analysis

Raw strain data were filtered using a 4th order zero lag Butterworth filter with a cutoff frequency of 125 Hz to attenuate noise in the signal. Data from 3–5 consecutive foot contacts were chosen for both the over-ground and treadmill trials in which the goat moved at a steady pace using a single gait. Typically, data from 50–60 strides were collected for each goat over the three gaits. The raw strain data were analyzed using a custom MATLAB program (The Mathworks, Inc.,

Natick, MA, USA) that zeroed and calibrated the data, converting voltages to microstrain (με, or strain $\times 10^{-6}$) based on a 1000 με shunt-calibration of the Vishay bridge amplifier. Zero strain levels were determined during the swing phase of the limb when the voltage change in the signal was minimal. Strain data for the rosette strain gauges were converted into principal strains, and their orientations determined using standard equations that assume a uniaxial planar state of strain (Biewener, 1992). Principal strains and strains recorded by the medial single element gauge were then adjusted ($=\varepsilon\times\mathbf{F}_v$ pre-surgery/$\mathbf{F}_v$ post-surgery) to correct for any post-surgical lameness in the limb, assuming that changes in strain were proportional to changes in limb loading. Post-operative forces were 80±9% (mean ± S.D.) of the pre-operative forces at a gallop (range, 63–95%), the gait for which the greatest post-operative sample sizes were obtained. Post-operative reductions in GRF of this magnitude are typical of strain gauge experiments examining mammalian forelimb bones (Biewener et al., 1983; Biewener and Taylor, 1986) and, although significant, the goats' gaits were not significantly altered. Thus, the reduction in limb load probably only affected strain magnitudes and not overall patterns or distributions of strain.

Peak positive (tensile) and negative (compressive) principal strains and their orientations, as well as peak tensile and compressive medial longitudinal strains and the percentage of stance phase when they occurred were determined. In keeping with previous studies (Rubin and Lanyon, 1982; Biewener and Taylor, 1986), the largest principal strains on the cranial and caudal surfaces, which were tensile and compressive, respectively, are those that we report and focus on in this study. The largest strains on the medial surface were compressive.

Peak axial and bending strains were determined using the following equations:

$$\varepsilon_{ax} = (\varepsilon_{cranial} + \varepsilon_{caudal})/2 , \quad (1)$$

$$\varepsilon_{b} = \pm|(\varepsilon_{cranial} + \varepsilon_{caudal})/2| . \quad (2)$$

The percentage of total strain in the radius due to bending was calculated as: $|\varepsilon_b|/(|\varepsilon_b|+|\varepsilon_{ax}|)\times 100$.

To gain a more detailed understanding of the strain environment in the midshaft of the radius and the position and orientation of the neutral axis of bending throughout the swing and stance phases, recordings from the central gauge axis of the cranial and caudal rosette gauges were used, together with longitudinal strains recorded by the single element gauge at the medial midshaft site, to determine the planar distribution of axial strains at the bone's midshaft (Biewener, 1992). This was mapped on the cross-section of the bone using a custom-written MATLAB program.

Bone geometry and percentage mineral content

Upon euthanization, both the left and right radii were removed from the limbs and cleaned of any muscle and connective tissue. The radii were then left to dry at room temperature for at least one week. Both the cranio-caudal (C-C) and medio-lateral (M-L) curvatures were measured from the non-instrumented (right) limb by dividing the radius of curvature for each direction by half the C-C or M-L diameter of the bone, respectively. The radius of curvature was measured as the orthogonal distance from the C-C or M-L midpoint of the bone at its midshaft to a line bisecting the proximal and distal articular ends of the bone (Bertram and Biewener, 1992).

The right radius was also used to determine the percentage mineral ash content. One-third of the bone's length, centered about the midshaft, was cut, and the periosteum, marrow and adjacent ulna removed and allowed to dry thoroughly. The bone section was weighed (Sartorius 1800; Goettingen, Germany), placed in a small aluminum dish, weighed again, and placed in an oven (Huppert Model 2 Deluxe; Chicago, IL, USA) for 12 h at 400°C. Immediately upon removal from the oven, the ashed bone and dish were weighed again. The percentage mineral ash content of the section of bone was determined as: post-ashed mass/pre-ashed mass × 100. Because adult goat ash specimens were limited, each middle third section of bone selected for ashing was cut in two and ashed separately. The mean of the two ash values was used in the analysis.

After measuring the alignment of the strain gauges and their placement relative to the bone's midshaft, the instrumented (left) radius and adjacent ulna were embedded in fiberglass resin (Bondo-Mar-Hyde Corp.; Atlanta, GA, USA). A 330 μm section was taken at the midshaft using a diamond annular saw (Microslice II; Cambridge Instruments, Ltd, Cambridge, UK). After affixing the section to a microscope slide, a magnified digital picture of the cross-section was taken using a video camera (Sony XC-75; Cypress, CA, USA). From this magnified cross-section, the cross-sectional area and C-C and M-L second moments of area (I_{CC} and I_{ML}, respectively) were calculated using a custom macro for NIH Image 1.61 (Bethesda, MD, USA). These measurements were also made including the ulna to determine to what extent it contributed to the forelimb skeleton's overall cross-sectional properties.

Statistical analyses

The means and standard deviations for the kinematic and strain data reported in the tables and throughout the text represent all the goats in a given size group for whom data were collected, based on individual mean values obtained from multiple trials (typically five) for each goat at a particular gait. The mean value for each trial was taken from the 3–5 foot contacts analyzed for that trial. Comparisons among different size groups and different gaits were analyzed using two-way analysis of variance (ANOVA; $P<0.05$; StatView 4.1; Abacus Concepts, Inc., Berkeley, CA, USA). Similarly, statistical comparisons testing for differences in limb loading through ontogeny were carried out using two-way ANOVA.

Least-squares regressions (KaleidaGraph 3.6; Synergy Software, Reading, PA, USA) were used to examine ontogenetic patterns of axial and bending strains *versus* speed and cross-sectional geometry, and percentage mineral ash content *versus* body mass. Significant differences in slope were

based on 95% confidence intervals derived from the regressions.

Results

Kinematic data

Duty factors, stride frequencies and stride lengths between the small and intermediate groups at each gait were not significantly different (P=0.96, P=0.61 and P=0.33, respectively; Table 1). Although the stride lengths observed in the adult goats during GRF data collection were significantly different from those observed in the two smaller groups at each gait (P<0.0001; Table 1), the duty factors and stride frequencies within each gait were not significantly different (P=0.90 and P=0.10, respectively). Because the duty factors were not significantly different, our comparisons of bone strain and limb loading across the three age/size groups therefore represent dynamically similar locomotor conditions.

Table 1. *Kinematic data – speed, duty factor, stride length and stride frequency*

	Walk	Trot	Gallop
Speed (m s^{-1})			
Small	0.83±0.17 (N=4)	1.66±0.25 (N=5)	2.34±0.47 (N=6)
Intermediate	0.85±0.15 (N=6)	1.73±0.33 (N=7)	2.74±0.41 (N=7)
Adult	1.21±0.10 (N=3)	2.27±0.15 (N=3)	3.59±0.41 (N=5)
Duty factor			
Small	0.58±0.02 (N=4)	0.45±0.03 (N=5)	0.35±0.03 (N=6)
Intermediate	0.59±0.04 (N=6)	0.46±0.08 (N=7)	0.33±0.05 (N=7)
Adult	0.60±0.02 (N=3)	0.44±0.03 (N=3)	0.32±0.02 (N=5)
Stride length (m)			
Small	0.41±0.05 (N=4)	0.56±0.03 (N=5)	0.73±0.11 (N=6)
Intermediate	0.45±0.05 (N=6)	0.60±0.06 (N=7)	0.85±0.08 (N=7)
Adult	0.76±0.03 (N=3)	0.96±0.04 (N=3)	1.30±0.13 (N=5)
Stride frequency (s^{-1})			
Small	2.05±0.23 (N=4)	2.96±0.39 (N=5)	3.23±0.40 (N=6)
Intermediate	1.97±0.29 (N=6)	2.86±0.31 (N=7)	3.22±0.21 (N=7)
Adult	1.56±0.09 (N=3)	2.37±0.05 (N=3)	2.78±0.23 (N=5)

Data (means ± S.D.) for the small and intermediate groups are from strain trials, while data for the adult group are from ground reaction force (GRF) trials. The mean speeds from the strain trials collected previously (Biewener and Taylor, 1986) and the adult GRF trials collected here were not significantly different (Student's paired t-tests, P>0.05).

Peak bone strains versus *size*

Peak midshaft bone strains in the radii of the two smaller groups were similar in distribution and alignment to those previously reported for the radius of adult goats. The dominant principal strain on the cranial surface (CR) was tensile (Table 2; Figs 1, 2A) and aligned primarily along the long axis of the bone in all gaits. On the caudal midshaft surface (CD), the larger principal strain was compressive (Table 2; Figs 1, 2B) and, despite greater variability among animals, was also generally aligned close to the long axis of the bone. Axial strains on the medial surface (MED) of the radius measured from single element strain gauges in the two smaller groups (but not previously in the adults; Biewener and Taylor, 1986) were also compressive (Table 2; Figs 1, 2C). In terms of absolute magnitude, strains measured in the small and intermediate animals were typically smallest at the cranial surface of the radius, larger at the caudal surface and largest at the medial surface.

Peak strains within the radius increased with an ontogenetic increase in body mass at all gauge locations across the three gaits. However, due to high inter-individual variation

Table 2. *Principal strains and orientation by size group and gait*

	Walk		Trot		Gallop	
	με	ϕ	με	ϕ	με	ϕ
Cranial						
Small	160±125 (N=4)	8±19 (N=4)	267±199 (N=5)	13±14 (N=5)	483±253 (N=5)	–7±19 (N=5)
Intermediate	435±185 (N=5)	12±16 (N=5)	591±249 (N=5)	–2±6 (N=5)	705±302 (N=5)	–9±18 (N=5)
Adult	653±171 (N=3)	4±18 (N=3)	1192±246 (N=3)	5±13 (N=3)	1316±79 (N=3)	4±12 (N=3)
Caudal						
Small	–329±138 (N=4)	18±39 (N=4)	–392±198 (N=4)	15±38 (N=4)	–593±334 (N=5)	16±26 (N=5)
Intermediate	–472±203 (N=4)	–26±38 (N=4)	–654±312 (N=4)	–3±8 (N=4)	–839±457 (N=4)	–1±5 (N=4)
Adult	–850±149 (N=3)	3±14 (N=3)	–1458±268 (N=3)	–2±14 (N=3)	–1647±214 (N=3)	–6±12 (N=3)
Medial						
Small	–516±49 (N=4)		–654±135 (N=5)		–774±329 (N=6)	
Intermediate	–535±268 (N=4)		–802±385 (N=4)		–929±425 (N=4)	

Data for the adult group were calculated from the raw data used in Biewener and Taylor (1986).
Values are means ± S.D.
με, microstrain (or strain ×10^{-6}); ϕ, orientation of the principal strain relative to the bone's long axis.

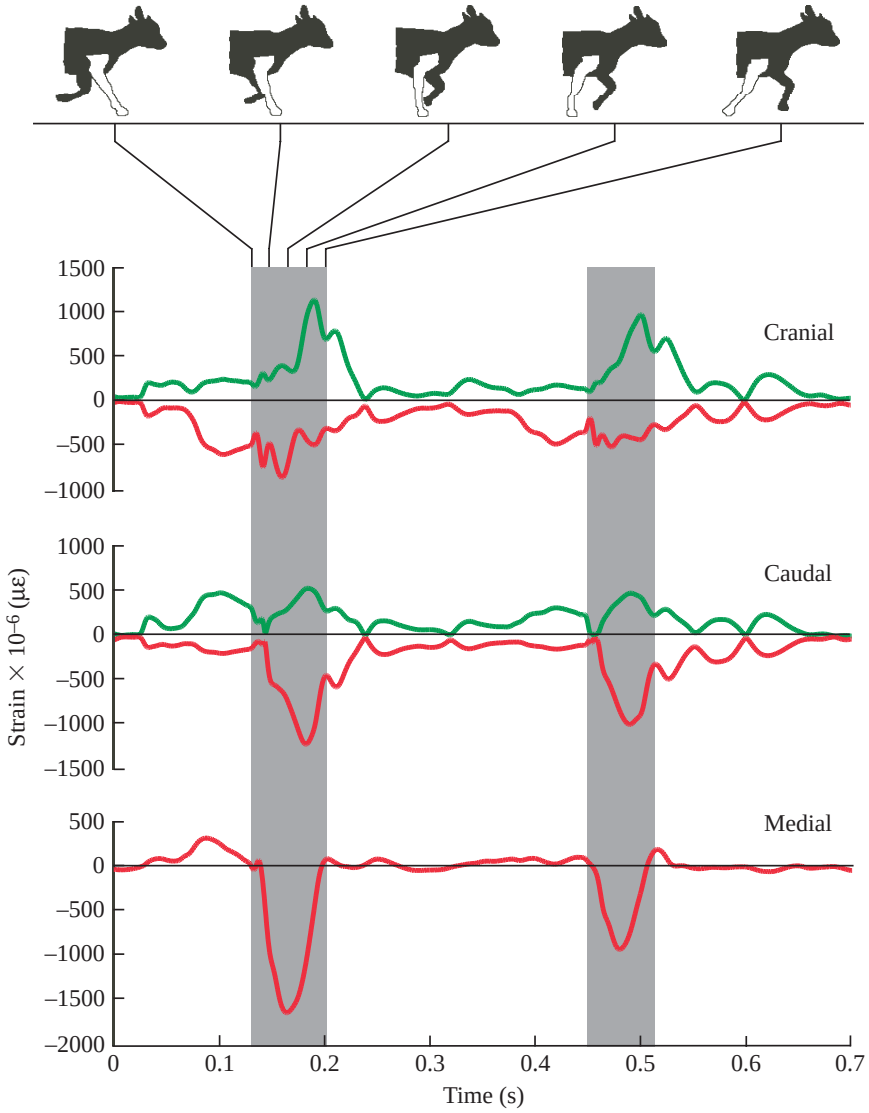

Fig. 1. Representative principal strains recorded from the cranial and caudal surfaces of the radius and axial strains from the medial surface for an intermediate-sized goat during two strides at a gallop (3.57 m s^{-1}). Principal tensile strains are in green and compressive (both principal and axial) strains are in red. Shaded bars represent the stance phase during the locomotor cycle. Silhouettes of the goat at the top show five phases during stance (0, 25, 50, 75 and 100%), with the recorded limb in white.

(Table 3), increases in peak strains within a gait between the small and intermediate groups were only significant on the cranial surface (CR, $P<0.01$; CD, $P=0.08$; MED, $P=0.36$). Peak strains in the adult radius, however, were significantly greater than those in the small and intermediate groups (CR and CD, $P<0.0001$).

Peak bone strains versus *gait*

Strains increased with speed and a change of gait at all three gauge locations (Table 2; Fig. 2) in the three groups. However, large inter-individual variation within the two smaller groups again resulted in the change in strain generally being insignificant between gaits (CR, $P=0.03$; CD, $P=0.11$; MED, $P=0.09$). In the adult goats, peak bone strains during trotting and galloping were significantly greater than those during walking, but no significant difference in peak strain was observed during trotting *versus* galloping (Biewener and Taylor, 1986).

Strains increased between 1.5- and 2-fold from a walk to a gallop at all three gauge sites in each size group, except on the cranial surface of the smallest group, where strains increased threefold from a walk to a gallop.

Axial versus *bending strain distributions in the radius*

Consistent with the overall increase in peak strain magnitude, both the axial (Fig. 3A) and bending (Fig. 3B) components of strain also increased with speed and change of gait. For axial compressive strains, this trend was significant in the smallest size group (slope, –60.8±22.5; 95% CI; $r^2=0.48$) but was not significant in the intermediate group due to the large variation among individuals (slope, –48.6±89.7; $r^2=0.04$; CV, 1.65±0.56). Nevertheless, the slopes of the regressions of axial compressive strain *versus* speed in the two groups were not significantly different from one another (based on their overlapping 95% CI). For strains due to bending, the slopes of the regressions describing the increase in bending across speed in the two groups were significant but again did not differ from one another (small, 241.3±58.8, $r^2=0.68$; intermediate, 147.2±53.0, $r^2=0.54$).

In all three size/age groups, bending constituted the major component of strain in the radius midshaft (Fig. 3C). This trend remained consistent across speed and gait (regression slopes of % bending strain were not significantly different from zero: small, 2.4±3.7, $r^2=0.05$; intermediate, 2.3±6.5, $r^2=0.02$; adult, see table 1 in Biewener and Taylor, 1986). In general, the radius of adult goats experienced the greatest amount of strain due to bending (mean, 89%; Biewener and Taylor, 1986), followed by the small group (73±9%) and then the intermediate group (70±18%).

Notably, the plane of bending was not static but typically shifted its orientation throughout stance (Fig. 4). The axial and bending strains reported in Fig. 3 occurred at the time of peak compressive and tensile strains on the caudal and cranial surfaces of the radius (73% of stance for the small group and 75% of stance for the intermediate group). At this time, the

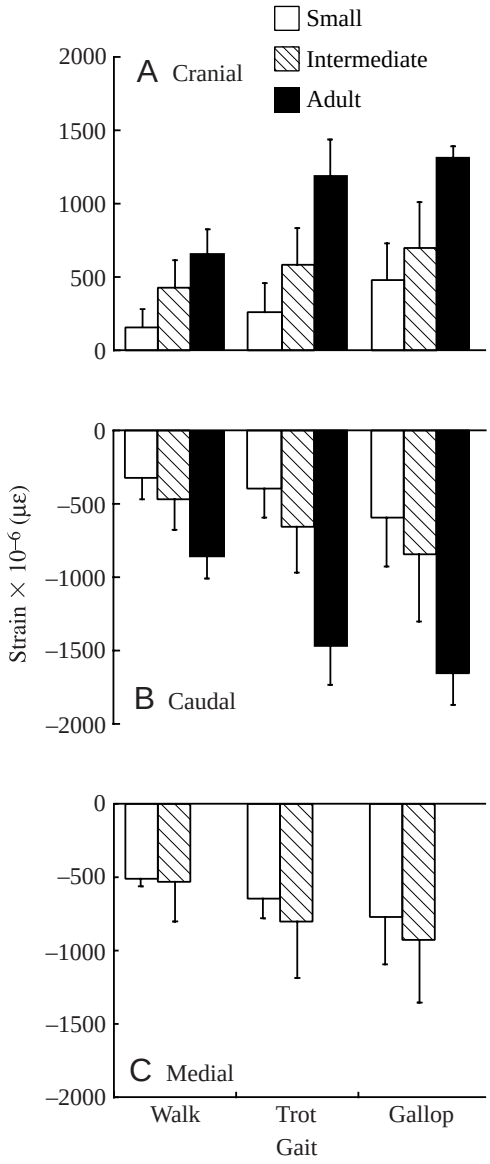

Fig. 2. Mean peak principal bone strains from the (A) cranial and (B) caudal surfaces, and (C) mean peak axial strains from the medial surface recorded at the midshaft of the radius for the small, intermediate and adult groups at a walk, trot and gallop. Error bars represent ±1 S.D. Medial axial strains are not present for the adult group, as they were not collected in Biewener and Taylor (1986).

orientation of bending was primarily in the cranio-caudal (C-C) direction with the neutral axis oriented in the medio-lateral (M-L) plane (Fig. 4D). However, at midstance, peak strains on the medial surface were typically, although not significantly, greater than those on the caudal surface, corresponding to a shift in the orientation of bending at this point in stance to the M-L direction (Fig. 4C). Because peak strains recorded on the medial surface were higher than those recorded on the cranial and caudal surfaces, M-L bending strains probably represented the maximum bending that the radius of the younger and smaller goats experienced.

Table 3. *Mean coefficients of variation (CV) for peak strains at each gauge location – within-individual variation and between-individual variation*

	Coefficient of variation	
	Within individual	Between individual
Cranial		
Small	0.18±0.05	0.68±0.14
Intermediate	0.14±0.04	0.42±0.00
Adult	0.13±0.02	0.18±0.10
Caudal		
Small	0.17±0.04	0.50±0.07
Intermediate	0.13±0.04	0.48±0.06
Adult	0.09±0.03	0.16±0.03
Medial		
Small	0.18±0.05	0.24±0.17
Intermediate	0.18±0.02	0.48±0.02

Data for the adult group are calculated from the raw data used in Biewener and Taylor (1986).
Values are means ± S.D.

Ontogenetic changes in limb loading

As expected, all three size/age groups showed a significant increase in the normalized vertical GRF exerted on the forelimb as animals increased speed and changed gait (Fig. 5; P=0.0001). However, no significant difference in normalized vertical limb load was observed over the speeds recorded within each gait among the three size classes (P=0.33). Consequently, within a given gait, the radius transmitted limb forces associated with the same relative ground reaction load regardless of size.

Bone curvature during ontogenetic growth

Both M-L and C-C normalized longitudinal curvatures of the radius did not change significantly throughout ontogeny (Fig. 6; regression slopes; M-L, 0.05±0.18, r^2=0.02; C-C, 0.12±0.14, r^2=0.13). Thus, the goat radius maintained its caudal and lateral concave curvatures during growth, with the C-C curvature exceeding the M-L curvature throughout ontogeny (1.04±0.25 *versus* 0.36±0.11, respectively; mean ± S.D.).

Ontogenetic changes in cross-sectional geometry

Strong patterns of negative allometry were observed in the ontogenetic scaling of the cross-sectional and second moments of area. Midshaft cross-sectional area of the radius scaled proportional to (body mass)$^{0.53\pm0.07}$ ($\propto M^{0.53\pm0.07}$, r^2=0.92; Fig. 7A). In goats, the ulna is closely associated with the radius, contributing 10.6% to the total cross-sectional area of these two skeletal elements of the forearm at the level of the midshaft of the radius. Although the ulna might, therefore, compensate for the relative decrease in cross-sectional area of the radius, the growth trajectory of the combined cross-sectional area of the radius and ulna at the level of the radial

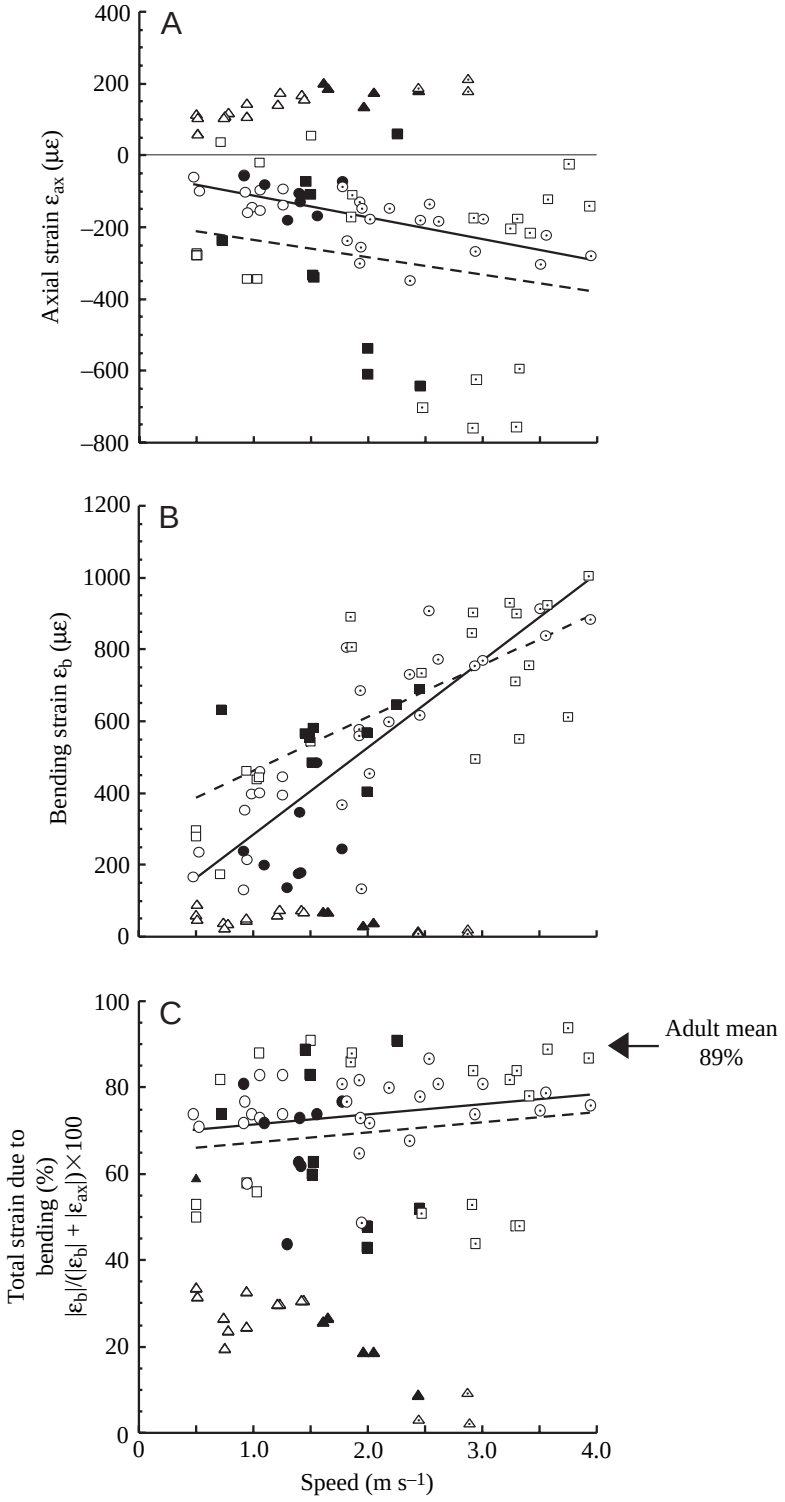

Fig. 3. Axial and bending strains in the radius determined from the cranio-caudal longitudinal principal strain data based on means for the individual trials at a given speed and gait for all small and intermediate animals. (A) Axial strain (ε_{ax}), (B) bending strain (ε_b) and (C) percentage of total strain due to bending plotted *versus* speed. Data for the small and intermediate groups are represented by circles and squares, respectively. Data for walking, trotting and galloping trials are represented by open, filled and open with a dot symbols, respectively. The solid regression line is fit to the data for the small group. The broken line is fit to the data for the intermediate group. In A, the equations of the regression lines (±95% CI for the slope, r^2) for the small and intermediate groups are y=–49.7–60.8x (±22.5, r^2=0.48) and y=–186.9–48.6x (±89.7, r^2=0.04), respectively. In B, small, y=44.3+241.3x (±58.8, r^2=0.68); intermediate, y=312.5+147.2x (±53.0, r^2=0.54). In C, small, y=69.0+2.4x (±3.7, r^2=0.05); intermediate, y=65.0+2.3x (±6.5, r^2=0.02). The mean percentage of strain due to bending observed for the adult group is indicated at 89% (Biewener and Taylor, 1986). Due to the large variation among individuals within each size/age group, trends from the small and intermediate groups are not significantly different. One goat from the small group (triangles) exhibited tensile axial strains and, although shown, was not included in the analyses of loading mode. The outlying tensile axial strains of this animal resulted from a strain distribution in which both the cranial and caudal surfaces were loaded in longitudinal tension and were near the neutral axis of bending, corresponding to the low strains that were recorded at the time of peak strain on the two surfaces.

midshaft exhibited the same negatively allometric scaling pattern ($\propto M^{0.52\pm0.07}$, r^2=0.91). Thus, both bone elements became reduced in size relative to the increase in body mass during ontogenetic growth.

Negative allometry of midshaft second moment of area of the radius scaled $\propto M^{1.03\pm0.12}$ (r^2=0.94) in the medio-lateral (I_{ML}) direction and $\propto M^{0.84\pm0.16}$ (r^2=0.85) in the cranio-caudal (I_{CC}) direction (Fig. 7B). As a result, the bone's resistance to bending, particularly in the cranio-caudal direction, was substantially reduced during growth. Once again, accounting for the ulna's contribution to bending resistance in the forearm resulted in only a slight change in the overall scaling of second moment of area for the two bone elements combined ($I_{ML}\propto M^{1.05\pm0.13}$, r^2=0.93; $I_{CC}\propto M^{0.80\pm0.16}$, r^2=0.83).

Ontogenetic changes in percentage mineral ash content

A small but significant increase in the percentage mineral ash content of the radial midshaft was observed through ontogeny (1 day to 7 years of age; Fig. 8; slope, 0.21±0.07, r^2=0.68), averaging 56.3±0.80% (N=10) in the smallest group, 57.3±1.21% (N=8) in the intermediate group and 59.1±1.29% (N=3) in the adult group.

Discussion

Ontogenetic changes in radial bone strain

The increase in strain magnitudes observed in the midshaft of the goat radius during growth from one size/age group to the next was unexpected. This pattern contradicted our first

hypothesis that strain magnitudes would remain constant through ontogeny, similar to the uniform strain patterns reported in the chick tibiotarsus (Biewener et al., 1986). Although strain magnitudes changed during growth, the strain distribution in the radius at the time of peak strain and the primary component of total strain (bending) was maintained during ontogeny, consistent with our third hypothesis. These observations are best explained by the interaction between ontogenetic patterns in both limb loading and geometric properties of bone morphology.

Counter to our second hypothesis that ontogenetic changes in bone shape would match ontogenetic changes in limb loading to maintain strain similarity, we found that the relative size and shape of the goat radius supporting these loads actually decreased. Strong negative allometry of cross-sectional area ($\propto M^{0.53}$) and second moments of area ($I_{CC} \propto M^{0.84}$; $I_{ML} \propto M^{1.03}$) of the radius clearly indicates a significant decrease in the capacity of the bone to support body-weight-related forces in both bending and axial compression. These forces probably remained uniform relative to the animal's size within each gait during ontogenetic growth. As a consequence, peak strain magnitudes increased with age and size when compared at dynamically similar gait speeds.

Negative allometry of the cross-sectional area of the radius was specifically correlated with increased axial compressive strains. It is not surprising based upon this trend alone that strains in the goat radius increased through ontogeny. However, in most tetrapod limb bones measured to date, which include the goat radius, bending strains are typically the major component of the total strain developed within the midshaft of a bone (Rubin and Lanyon, 1982; Biewener and Taylor, 1986; Biewener, 1991). Thus, the strong negative allometry of the second moments of area in the goat radius, which substantially reduced its capacity for resisting bending moments in the C-C and M-L directions, explains most of the observed increase in locomotor strains as the goats grew in size and weight. The bone's greater negative allometry and increased susceptibility to bending in the C-C direction relative to the M-L direction is somewhat surprising, given its greater C-C curvature and the parasagittal motion of the limb during locomotion.

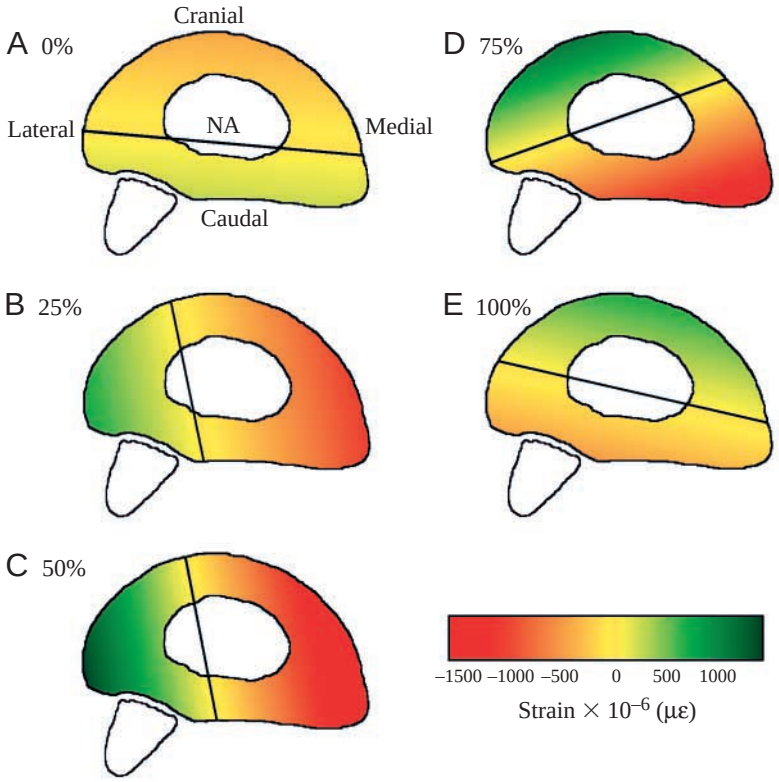

Fig. 4. Cross-sectional longitudinal strain distributions in the radius from the same intermediate-sized goat during a gallop (3.57 m s^{-1}) as shown in Fig. 1. Five phases are shown as percentage of time through stance: (A) 0%, (B) 25%, (C) 50%, (D) 75% and (E) 100%. Anatomical axes are labeled in A. The position of the neutral axis is indicated by the heavy black line. The outline of the ulna is included for reference, located caudo-lateral to the radius. The scale for the color gradient goes from red for negative (compressive) strains to yellow near zero strain and toward green for positive (tensile) strains.

Increased load predictability in the radius through ontogeny

Engineered structures are typically built to minimize deflection or bending under a habitual load, so it is counterintuitive that the goat radius is predisposed throughout ontogeny to be bent in the C-C direction. The interaction between bone curvature and asymmetric cross-sectional geometry favoring a preferential bending direction has been hypothesized to improve a bone's 'load predictability' (Bertram and Biewener, 1988). According to this hypothesis, a long bone's form evolves to meet the conflicting demands for strength *versus* strain predictability as animals subject their

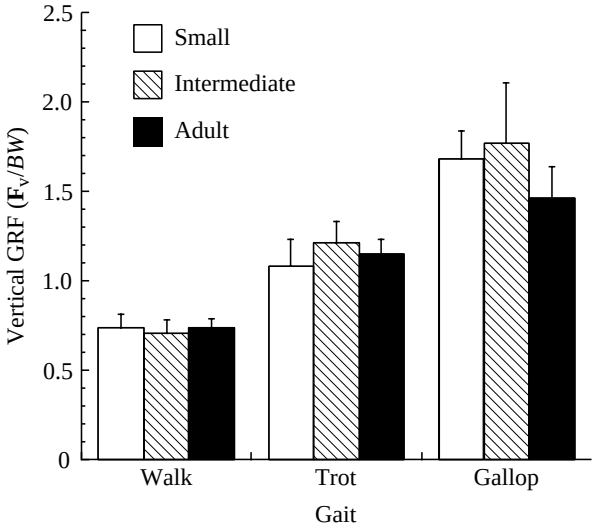

Fig. 5. Normalized peak vertical ground reaction forces (GRF) against gait for the small, intermediate and adult groups. Peak vertical forces ($\mathbf{F}_v$) were normalized by dividing the forces by the body weight (*BW*) of the goat. Error bars represent ±1 S.D.

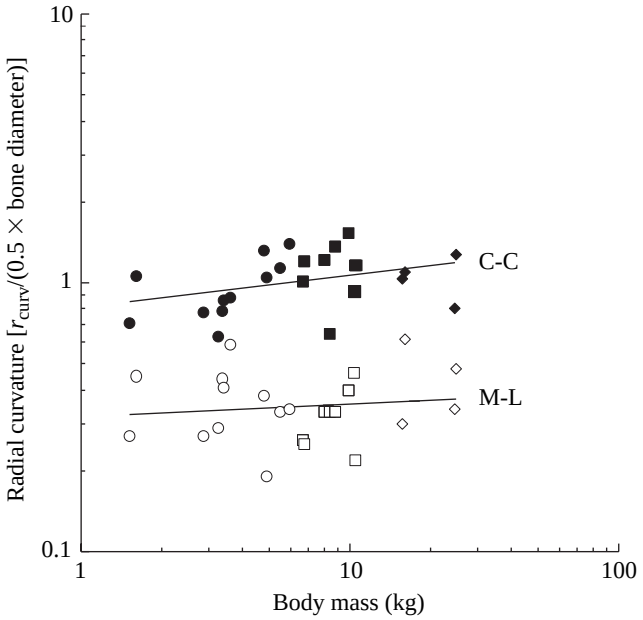

Fig. 6. Cranio-caudal and medio-lateral longitudinal curvature of the radius plotted against body mass on logarithmic axes. Data for the small, intermediate and adult groups are represented by circles, squares and diamonds, respectively. Cranio-caudal (C-C) and medio-lateral (M-L) data are represented by filled and open symbols, respectively. C-C, $y=0.81x^{0.12\pm0.14}$ ($r^2=0.13$); M-L, $y=0.32x^{0.05\pm0.18}$ ($r^2=0.02$).

bones to variable loading conditions. This seems to reflect the growth pattern and increased cross-sectional shape asymmetry of the goat radius. Its relative decrease in second moment of area in the C-C direction, combined with its greater curvature in this direction, favors an increase in bending-induced strains in the C-C cortices during growth, as was generally observed. At the same time, this may provide the bone with increased loading predictability (Lanyon, 1987; Bertram and Biewener, 1988).

Consistent with preferential C-C bending, the muscles that span and transmit loads *via* the radius lie mainly in the C-C plane of the bone. Depending on when certain muscle groups are active, this musculoskeletal organization could either augment or attenuate the C-C bending moments imposed upon the limb by the GRF (Pauwels, 1980). Although strains were not measured on either the medial or lateral surfaces of the adult goat radius (Biewener and Taylor, 1986), in the younger groups examined here strains recorded on the medial surface were largest, despite the bone's greater resistance to bending in the M-L direction. This suggests that, whereas muscles arranged along the C-C surfaces of the radius could serve to control and attenuate strains in these cortices, resistance to bending in the M-L plane is wholly reliant upon the bone's inherent flexural stiffness.

Ontogenetic changes in bone material properties

The flexural stiffness of a bone is not only dependent upon its second moment of area but also its elastic modulus (E).

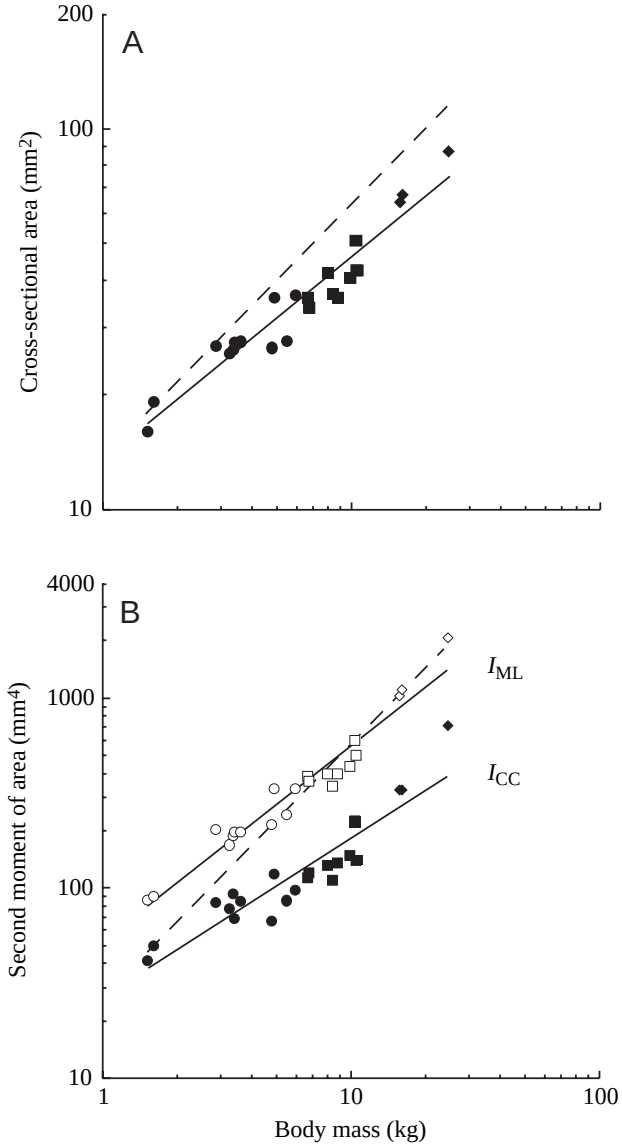

Fig. 7. (A) Cross-sectional area and (B) cranio-caudal and medio-lateral second moments of area (I) of the radius at the midshaft plotted against body mass on logarithmic axes. Data for the small, intermediate and adult groups are represented by circles, squares and diamonds, respectively. Cranio-caudal (I_{CC}) and medio-lateral (I_{ML}) data are represented by filled and open symbols, respectively. In A, $y=13.4x^{0.53\pm0.07}$ ($r^2=0.92$). In B, I_{CC}, $y=26.6x^{0.84\pm0.16}$ ($r^2=0.85$); I_{ML}, $y=52.3x^{1.03\pm0.12}$ ($r^2=0.94$). The broken lines represent isometry in each case (slope: A, 0.67; B, 1.33) and are positioned to facilitate comparison with the regression lines (solid lines).

Elastic modulus depends on the degree of bone mineralization, with older, more highly mineralized bone tissue typically having a higher modulus (Currey and Pond, 1989; Brear et al., 1990; Currey, 1999). Using simple beam theory, $\varepsilon_b=By/EI$, where B is the applied bending moment and y is the bone's radius (Wainwright et al., 1976), we predict that E would need to increase by 1.77 times from small to adult goats to maintain uniform C-C bending strains in the radius during ontogeny.

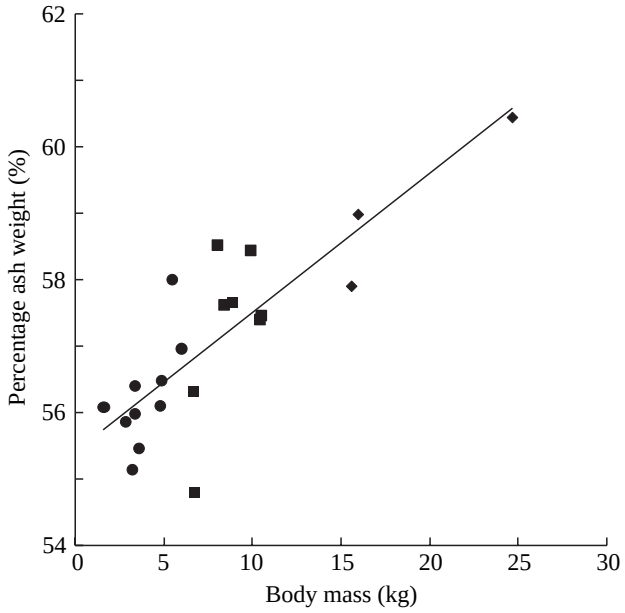

Fig. 8. Percentage mineral ash weight against body mass. Data from the small, intermediate and adult groups are represented by circles, squares and diamonds, respectively. y=55.4+0.21x (±0.07, r^2=0.68).

Lanyon et al. (1979) found that, in the sheep radius, E increased by 1.27 times for a 2.1% increase in percent ash content from 17 weeks to >4 years of age, suggesting that the 2.8% ash increase we observed in the goat radius, although providing some increase in bending resistance, did not increase E sufficiently to maintain peak strain levels uniform during ontogeny.

Although the small increase in mineralization (and, by extension, elastic modulus) and strong negative allometry suggest that the adult goat radius may be increasingly under-built as it grows, peak strains developed in the adult radius at a gallop (–1850 με; Biewener and Taylor, 1986) are no larger than those reported for most other vertebrates measured to date, which usually range between –1800 με and –3000 με (Rubin and Lanyon, 1982). Therefore, it seems more likely that the radii of adult goats are not under-built but, rather, the radii of young goats are over-built.

Ecological and evolutionary factors influencing the growth trajectory of the goat radius

Goats are precocial animals that live in herds that include both adult and juvenile individuals. Their collective movements therefore require that young animals, with shorter legs, take many more steps and maintain a relatively faster speed to keep up with the adults in the herd. In the present study, we observed that adult goats had a stride length of 0.76 m when they walked at a speed of 1.21 m s^{-1} (Table 1). At this speed, a young goat corresponding to our small size group would need to trot slowly to keep up with an adult, subjecting its limbs to a higher frequency of greater loads and strains. To maintain pace with a trotting adult (2.27 m s^{-1}), a young goat would have to gallop (2.34 m s^{-1}; Table 1). Given that peak strains in the radius of the young goats at a gallop were only about 70% of those in a walking adult goat, there is therefore no substantial mechanical detriment for a young goat having to gallop to keep up with the adults. Even though the radius of the young goats at a gallop supports 1.7BW while the adult radius at a walk supports only 0.7BW, the relatively greater cross-sectional area and second moments of area of the younger goat radius maintain strains at comparably safe levels, even when the young goats move quickly for their size.

The ‘over-design’ of the radius at a young age may not only help young goats to literally ‘keep up with the herd’ but may also provide a greater safety factor during their first days following birth, when their movements may be less well coordinated and unstable. This might produce more variable patterns of bone loading, consistent with the generally greater within-individual variation in peak strains that we observed in younger goats (Table 3). With growth, the need for an enhanced safety factor diminishes as an older goat’s stride length increases and they become more adept at walking and running. At this stage, the cost of maintaining a relatively ‘over-built’ radius may outweigh the risk of mechanical failure in the radius, which becomes loaded in a more predictable manner as the goats grow and mature. Thus, the ontogenetic growth patterns in the radius seem to correspond well to changing mechanical demands in the goat’s life history.

Finally, the terrain itself may present a more variable substrate for a younger, smaller goat, possibly causing them to encounter a wider variety of limb and bone loading. The less eccentric cross-sectional geometry and increased area and second moments of area of the radius of young relative to adult goats seem consistent with this. This would favor the much lower, but more variable, strains that we observed during steady level locomotion. Under less steady conditions and more varied terrain, bone strain levels might be even more variable and of greater magnitude.

Ontogenetic strain patterns in the goat radius versus *the chicken tibiotarsus*

In the only other study that has examined ontogenetic patterns of bone strain, Biewener et al. (1986) found that locomotor strains in the chicken tibiotarsus generally remained uniform throughout ontogeny. Chickens are also precocial animals and are capable of body support and locomotor movement soon after hatching. Similar to the pattern of ontogenetic growth observed for the goat radius, the cross-sectional area ($\propto M^{0.55}$) and second moment of area ($\propto M^{1.22}$) of the tibiotarsus also scaled with negative allometry, well below what would be expected to maintain strains at similar levels (Biewener and Bertram, 1994). However, because this earlier study did not examine patterns of limb loading, it is difficult to assess the basis for strain similarity observed during growth of the chicken tibiotarsus. These observations would appear to suggest that older chickens experience lower relative limb loads at functionally equivalent speeds.

The results obtained for the goat radius in comparison with the chicken tibiotarsus show that similar ontogenetic patterns

of bone growth can result in varying ontogenetic patterns of bone strain. This suggests that differences in a species' ontogeny and locomotor capability can have important influences on bone growth and bone loading, which may allow juvenile animals to achieve absolute performance levels similar to those of adults (Carrier, 1983). Further examination of limb bone growth patterns in a wider diversity of taxa is needed to better understand the interplay among ontogenetic patterns of bone growth, limb loading and locomotor capacity in relation to a species' ecology and evolutionary history. Studies of *in vivo* bone strain patterns under more variable, natural conditions are also needed to evaluate how variation in locomotor activity affects the distribution and pattern of strain within a bone, as well as how the magnitude and pattern of strain change during growth.

We would like to thank Pedro Ramirez for animal care, Anna Ahn, Monica Daley, Colleen Donovan, Gary Gillis, Joyce Main, Craig McGowan, Rebecca Mitchell, Ryan Monti, Stephanie Schur and Jim Usherwood for assistance during different phases of the experiments, and Ty Hedrick for assistance in writing the MATLAB programs. This work was supported in part by the Chapman Fund (Harvard University).

References

Alexander, R. McN. (1981). Factors of safety in the structure of animals. *Sci. Prog. Oxf.* **67**, 109-130.

Alexander, R. McN., Jayes, A. S., Maloiy, G. M. O. and Wathuta, E. M. (1979). Allometry of the limb bones of mammals from shrews (*Sorex*) to elephant (*Loxodonta*). *J. Zool. Lond.* **189**, 305-314.

Bertram, J. E. A. and Biewener, A. A. (1988). Bone curvature: sacrificing bone strength for load predictability? *J. Theor. Biol.* **131**, 75-92.

Bertram, J. E. A. and Biewener, A. A. (1992). Allometry and curvature in the long bones of quadrupedal mammals. *J. Zool. Lond.* **226**, 455-467.

Biewener, A. A. (1982). Bone strength in small mammals and bipedal birds: do safety factors change with body size? *J. Exp. Biol.* **98**, 289-301.

Biewener, A. A. (1983). Allometry of quadrupedal locomotion: the scaling of duty factor, bone curvature and limb orientation to body size. *J. Exp. Biol.* **105**, 147-171.

Biewener, A. A. (1989). Scaling body support in mammals: limb posture and muscle mechanics. *Science* **245**, 45-48.

Biewener, A. A. (1991). Musculoskeletal design in relation to body size. *J. Biomech.* **24**, 19-29.

Biewener, A. A. (1992). *In vivo* measurement of bone strain and tendon force. In *Biomechanics – Structures and Systems* (ed. A. A. Biewener), pp. 123-147. New York: Oxford University Press.

Biewener, A. A. and Bertram, J. E. A. (1994). Structural response of growing bone to exercise and disuse. *J. Appl. Physiol.* **76**, 946-955.

Biewener, A. A. and Dial, K. P. (1995). *In vivo* strain in the humerus of pigeons (*Columba livia*) during flight. *J. Morph.* **225**, 61-75.

Biewener, A. A. and Taylor, C. R. (1986). Bone strain: a determinant of gait and speed? *J. Exp. Biol.* **123**, 383-400.

Biewener, A. A., Thomason, J. and Lanyon, L. E. (1983). Mechanics of locomotion and jumping in the horse (*Equus*): *in vivo* stress developed in the radius and metacarpus. *J. Zool. Lond.* **201**, 67-82.

Biewener, A. A., Swartz, S. M. and Bertram, J. E. A. (1986). Bone modeling during growth: dynamic strain equilibrium in the chick tibiotarsus. *Calcif. Tissue Int.* **39**, 390-395.

Blob, R. W. and Biewener, A. A. (1999). *In vivo* locomotor strain in the hindlimb bones of *Alligator mississippiensis* and *Iguana iguana*: implications for the evolution of limb bone safety factor and non-sprawling limb posture. *J. Exp. Biol.* **202**, 1023-1046.

Brear, K., Currey, J. D. and Pond, C. M. (1990). Ontogenetic changes in the mechanical properties of the femur of the polar bear *Ursus maritimus*. *J. Zool. Lond.* **222**, 49-58.

Carrier, D. (1983). Postnatal ontogeny of the musculo-skeletal system in the black-tailed jack rabbit (*Lepus californicus*). *J. Zool. Lond.* **201**, 27-55.

Carrier, D. and Leon, L. R. (1990). Skeletal growth in the California gull (*Larus californicus*). *J. Zool. Lond.* **222**, 375-389.

Currey, J. D. (1999). What determines the bending strength of compact bone? *J. Exp. Biol.* **202**, 2495-2503.

Currey, J. D. and Pond, C. M. (1989). Mechanical properties of very young bone in the axis deer (*Axis axis*) and humans. *J. Zool. Lond.* **218**, 59-67.

Lanyon, L. E. (1987). Functional strain in bone tissue as an objective, and controlling stimulus for adaptive bone remodelling. *J. Biomech.* **20**, 1083-1093.

Lanyon, L. E., Magee, P. T. and Baggott, D. G. (1979). The relationship of functional stress and strain to the processes of bone remodelling. An experimental study on the sheep radius. *J. Biomech.* **12**, 593-600.

Maloiy, G. M. O., Alexander, R. McN., Njau, R. and Jayes, A. S. (1979). Allometry of the legs of running birds. *J. Zool. Lond.* **187**, 161-167.

Pauwels, F. (1980). *Biomechanics of the Locomotor Apparatus*. New York: Springer-Verlag.

Rubin, C. T. and Lanyon, L. E. (1982). Limb mechanics as a function of speed and gait: a study of functional strains in the radius and tibia of horse and dog. *J. Exp. Biol.* **101**, 187-211.

Swartz, S. M., Bennett, M. B. and Carrier, D. R. (1992). Wing bone stresses in free flying bats and the evolution of skeletal design for flight. *Nature* **359**, 726-729.

Wainwright, S. A., Biggs, W. D., Currey, J. D. and Gosline, J. M. (1976). *Mechanical Design in Organisms.* Princeton: Princeton University Press.